Supporting Information Available

Table of Contents

SI-1: Control experiment - collagen mineralization without supplements

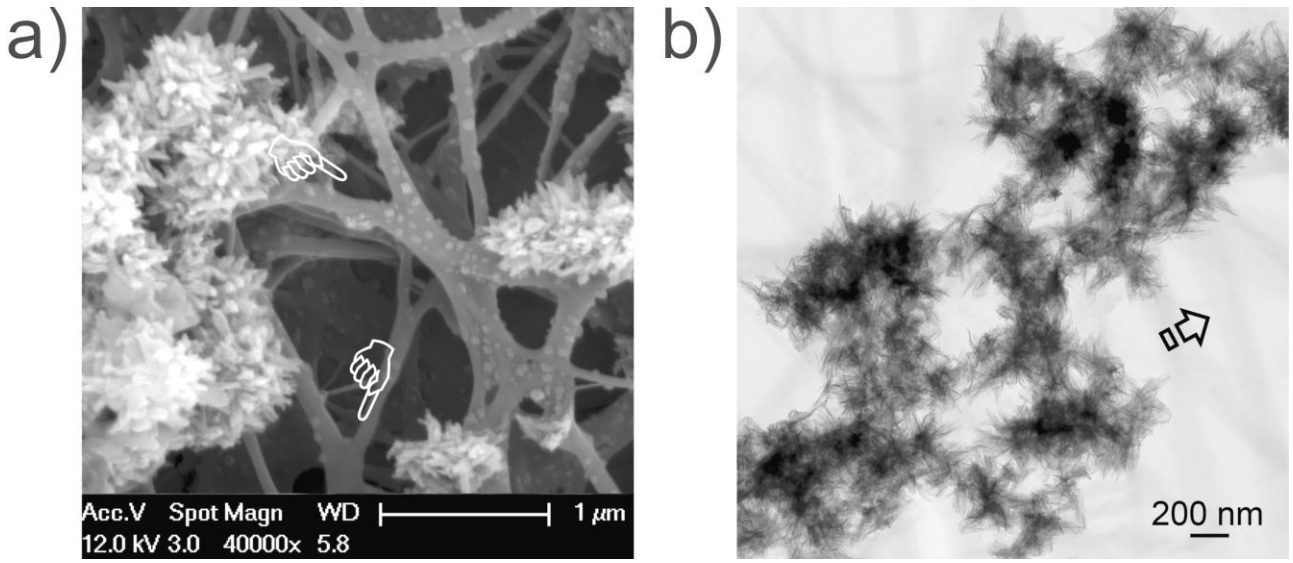

SEM and unstained TEM images of the control in which reconstituted collagen without TPP treatment was immersed in the mineralizing composite/simulated body fluid system without inclusion of PAA as the ACP stabilization agent. **a)** SEM taken at 72 h showing spherules of circumferentially protruding apatite crystals around the collagen matrix. **b)** TEM taken at 72 h showing almost complete transformation of amorphous calcium phosphate spheres into apatite crystals. There is no mineralization of the adjacent collagen fibrils (open arrow).

SI-2: Collagen mineralization after TPP sorption but without PAA supplement in the simulated body fluid

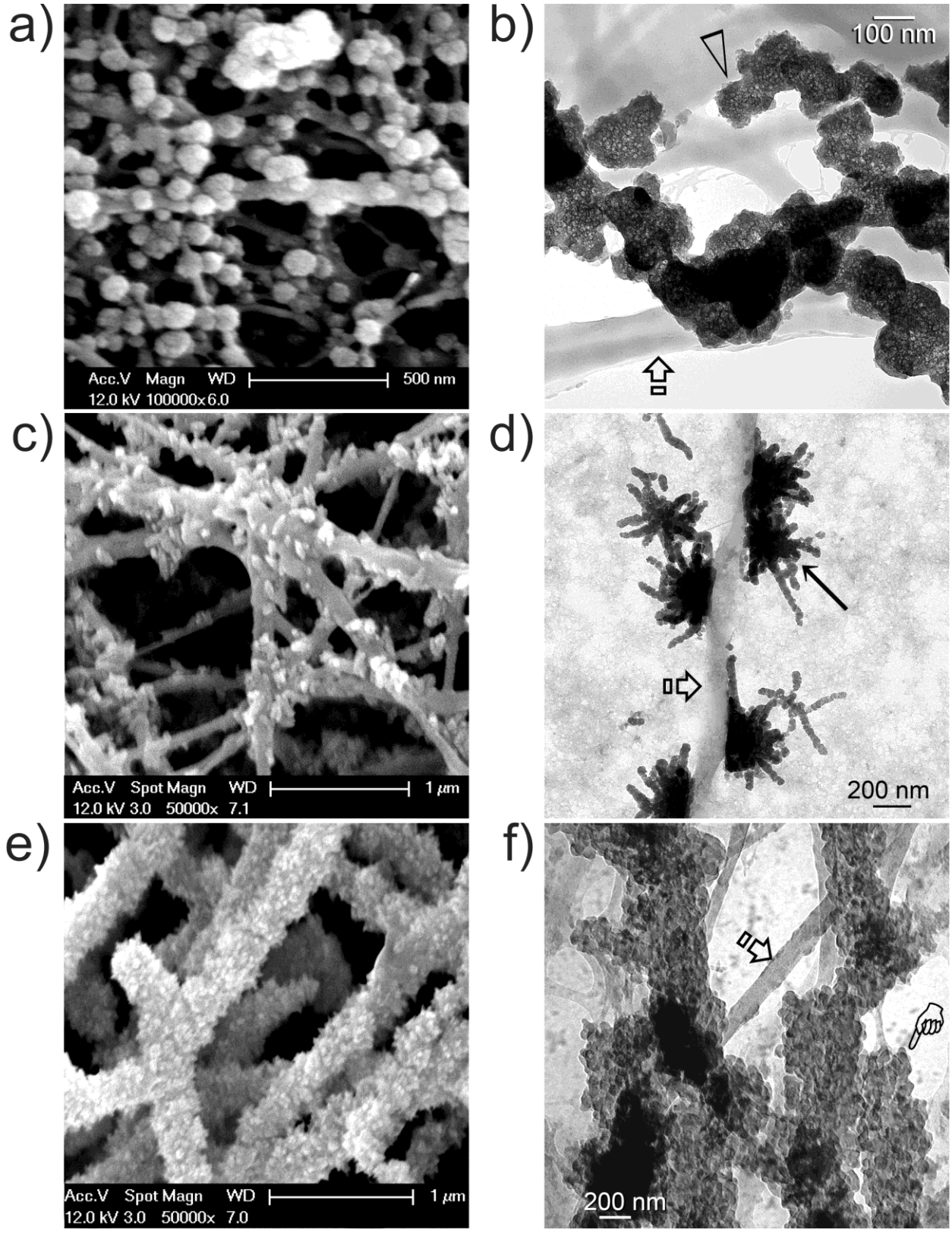

a) SEM and **b)** unstained TEM images showing different stages of extrafibrillar mineralization in which reconstituted collagen treated with 0.245 M TPP were immersed in simulated body fluid without PAA as the ACP stabilization agent. Precipitation of the inorganic phase over the surface of the organic phase does not result in a genuine nanocomposite. **a)** SEM showing ACP spheres aggregating to the surface of collagen fibrils after 4 h of mineralization. **b)** Corresponding TEM of a collagen-coated TEM grid showing ACP aggregates (open arrowheads) in the vicinity of non-mineralized collagen fibrils (open arrow). The latter were devoid of cross-banding patterns (open arrow). Stabilization of ACP in the absence of PAA, albeit inadequate, may be due to the surfactant property of TPP [S1] as it partial desorbed from the collagen fibrils. **c**) SEM taken after 24 h of mineralization showing amorphous-crystalline transition of the original ACP aggregates. **d**) Corresponding TEM showing transformation of ACPs into immature crystalline phases (arrow) along the surface of the non-mineralized collagen fibril (open arrow). **e)** SEM taken after 72 h of mineralization showing complete coating of the collagen fibrils with extrafibrillar apatite aggregates. **f)** Corresponding TEM showing thick collagen fibrils that were coated with extrafibrillar crystalline platelets (pointer). Open arrow: non-mineralized collagen fibrils.

SI-3: Ultrastructural features of the ACP infiltration stage of collagen-apatite assembly

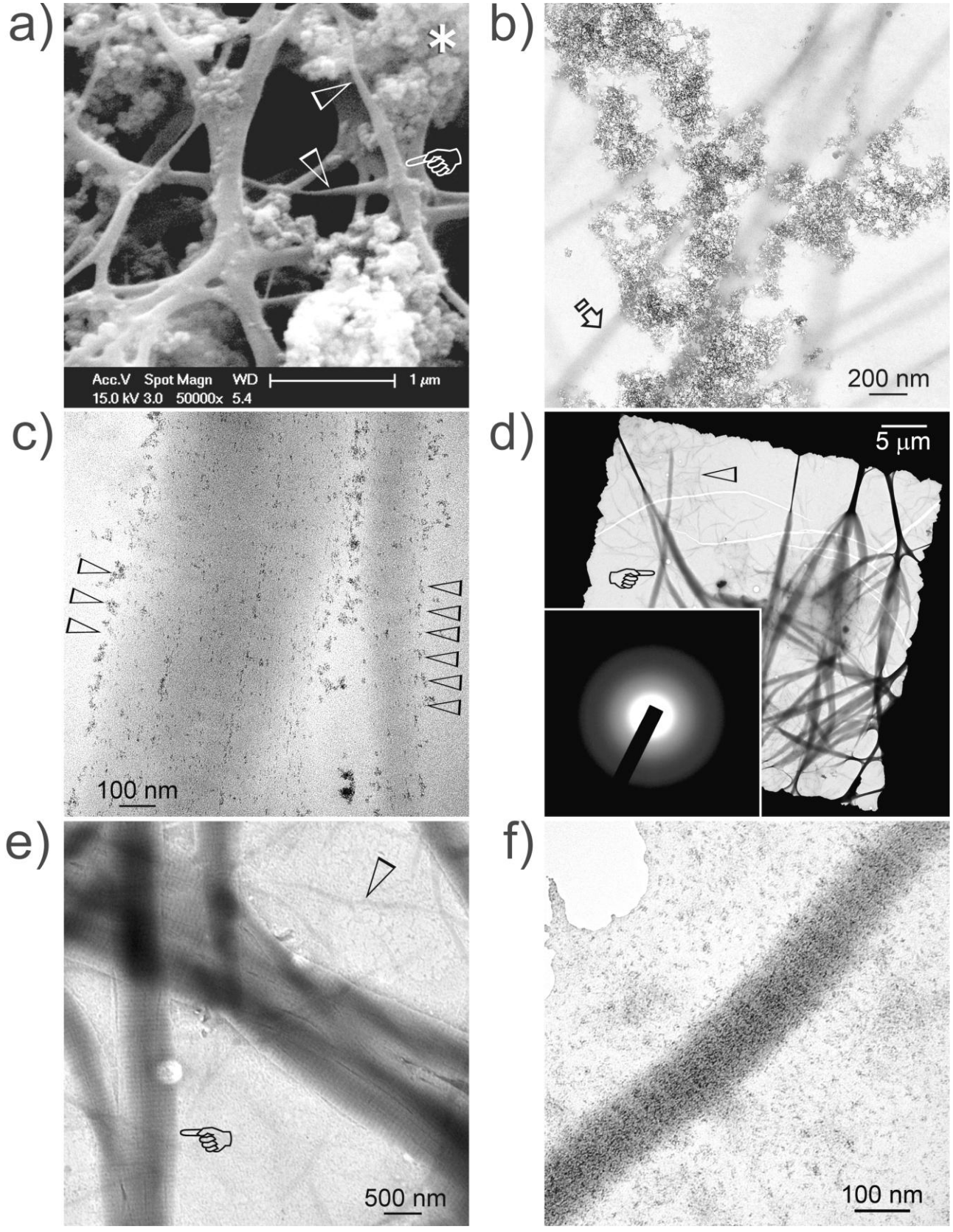

a) SEM and **b)** unstained TEM images showing the "ACP infiltration stage" of nanocomposite assembly at 4-24 h in the presence of PAA as the ACP stabilization agent. Reconstituted collagen matrices for both SEM (3 mg/mL) and TEM (0.2 mg/mL) were treated with 0.245 M TPP for 1 h prior to immersion in the mineralization medium. **a)** SEM of a 3-D collagen matrix showing aggregation of ACP mesophases (asterisk) around collagen fibrils. Some fibrils appeared swollen with vaguely discernible cross-banding patterns (pointer). Non-swollen regions are present along the same fibrils (open arrowheads). The apparent swelling is due to the intrafibrillar minerals resisting dehydration shrinkage. **b)** TEM taken at 4 h showing aggregation of ACP mesophases around non-mineralized collagen fibrils (open arrow). **c)** At 12 h, calcium phosphate prenucleation clusters are attracted to the fibrillar surface. Their locations corresponded approximately to the ≈ 67 nm D-spacing of the collagen fibrils. This image shows two collagen fibrils with periodically-attached calcium phosphate prenucleation clusters (open arrowheads). A more detailed presentation of these prenucleation clusters is given in Supporting Information SI-6. **d)** Between 12-24 h, fibrils are infiltrated with electron-dense, amorphous ACP. Inset: selected area electron diffraction indicates that the infiltrated mineral phase is amorphous. Open arrowhead: non-swollen fibril. **e)** High magnification of **d)** showing ACP-infiltrated (pointer; ca. 200-300 nm) and non-infiltrated fibrils (open arrowhead). **f)** At 24 h, electron-dense nucleation sites appear within some of the ACP-infiltrated fibrils, which return to their original dimensions (50-100 nm) probably as a result of the loss of water of hydration from the amorphous mineral phase. The mineral phase within these fibrils remains amorphous at this stage.

SI-4: Ultrastructural features of the calcium phosphate prenucleation clusters and ACP aggregates formed around collagen fibrils

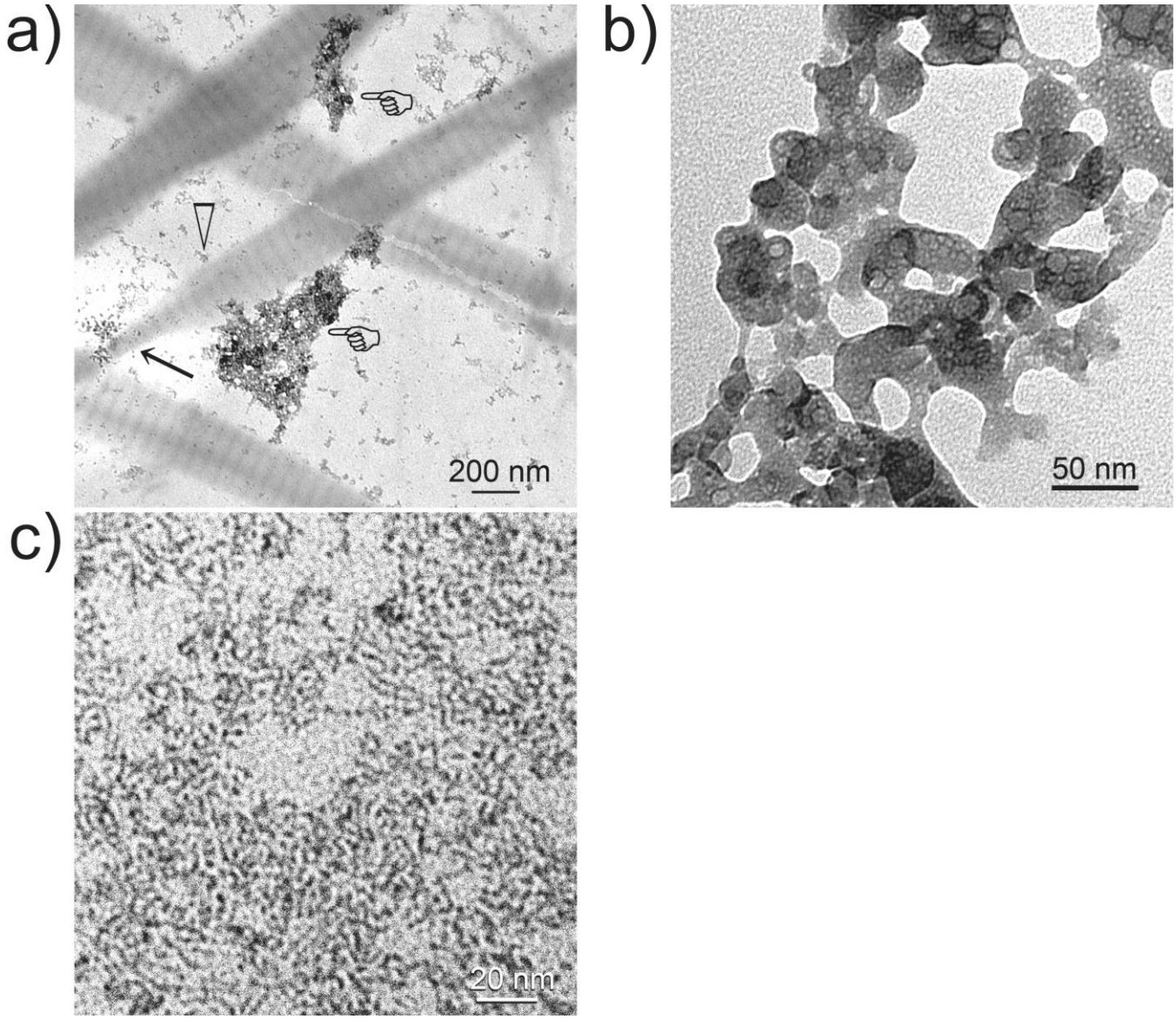

Unstained TEM images of prenucleation clusters[S2,S3] and ACP aggregates stabilized by polyacrylic acid. **a)** Larger ACP aggregates that coalesce in the vicinity of the collagen fibrils but do not infiltrate the fibrils (pointer). Smaller prenucleation clusters are attached to the surface of the collagen fibrils (open arrowhead) and infiltrate the internal compartments of the collagen fibril. Note the transition from a non-swollen to a swollen fibril (arrow). **b)** High magnification of the larger, partially-coalesced ACP aggregates that are in the 20-50 nm range. **c)** High magnification of the calcium phosphate prenucleation clusters that are formed in solution and subsequently attached to the surface of collagen fibrils (see SI-3C). Each unit within the prenucleation cluster is in the range of 1 nm.

SI-5: Initial apatite nucleation sites at the ACP infiltration stage

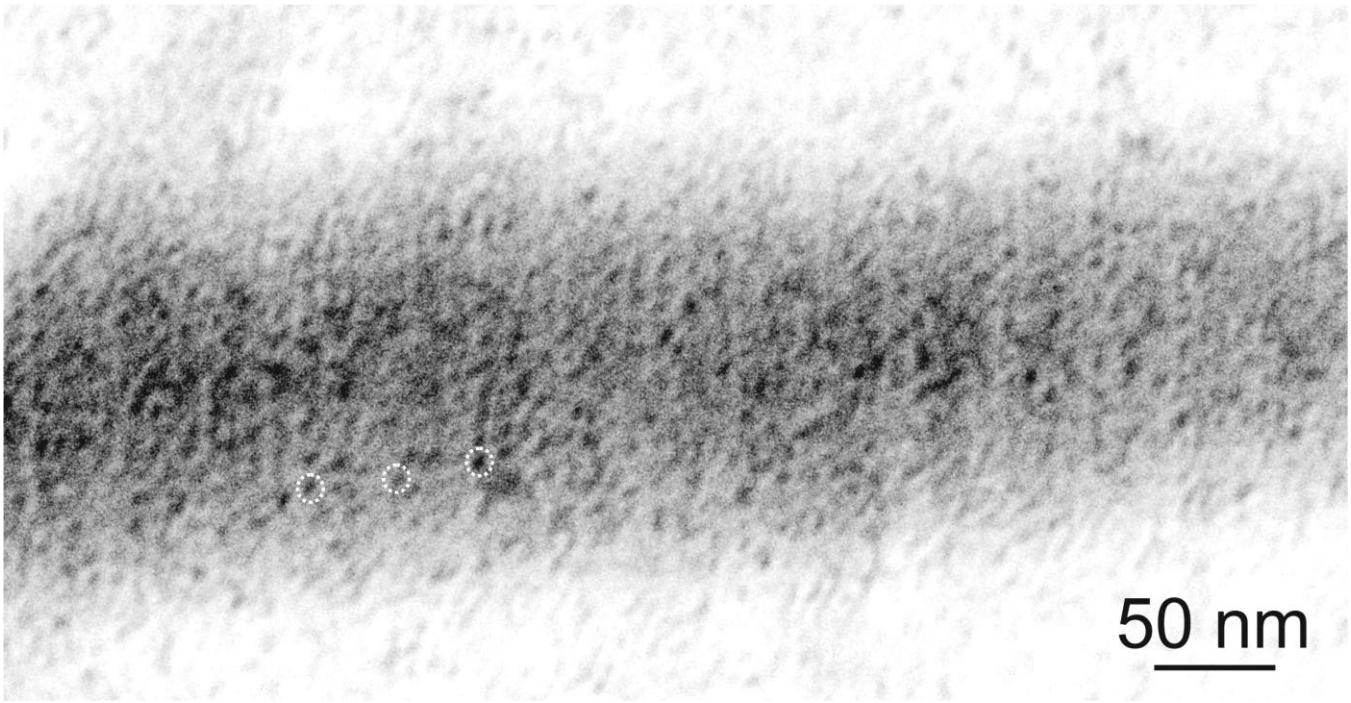

Unstained (gamma-adjusted) high magnification image of a collagen fibril similar to the one depicted in **SI-3f** showing electron-dense spots (e.g. those enclosed by dotted circles) that are probably niduses of nucleation within the coalesced amorphous calcium phosphate phase. Periodic alignment of these potential nucleation sites in a direction perpendicular to the longitudinal axis of the collagen fibril enables cross-banding patterns to be vaguely discerned in the absence of staining.

SI-6: FT-IR of mineralized collagen matrices retrieved after 72 h of mineralization

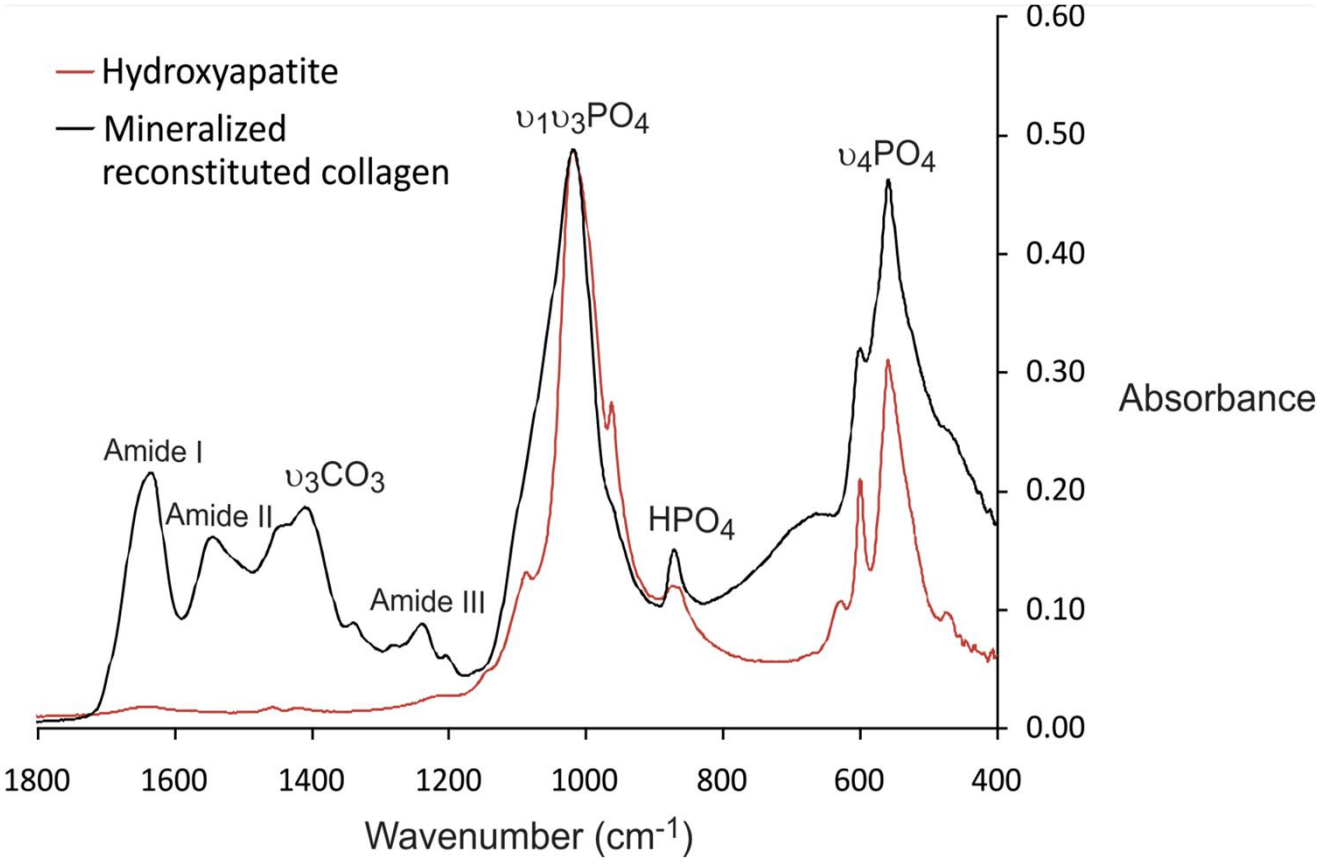

Infrared spectra of commercially available hydroxyapatite (Sigma-Aldrich) and mineralized reconstituted collagen matrices (3 mg/mL) that are treated with 0.245 M TPP for 1 h and immersed in simulated fluid containing 0.28 mM PAA confirm that the minerals formed in the inorganic-organic nanocomposite are apatite. The spectra are normalized against the peak assigned to the υ_3 P-O stretching mode of hydroxyapatite at 1020 cm^{-1}. The peak at 960 cm^{-1} is assigned to the υ_3 P-O stretching mode of hydroxyapatite. Peaks at 602 and 562 cm^{-1} are assigned to the υ_4 O-P-O bending mode of hydroxyapatite. The peak at 1413 cm^{-1} is assigned to the υ_3 C-O stretching mode of carbonate substitution in the apatite lattice. The peak at 872 cm^{-1} is assigned to HPO_4 substitution in the apatite lattice.[S4] Peaks at ≈ 1650, 1550 and 1250 cm^{-1} (thin arrows) are assigned respectively to the amide I, II and III bands of type I collagen. Note that analytical techniques such as FT-IR, energy-dispersive X-ray analysis, X-ray diffraction or thermogravimetric analysis do not provide information on whether the inorganic phase is located within the organic phase in the form of a nanocomposite. Confirmation of the presence of an intrafibrillar mineral phase can only be achieved using TEM or observations of meridional reflections produced by small-angle x-ray scattering.

SI-7: X-ray diffraction of pulverized mineralized collagen matrices retrieved after 72 h of mineralization

A. Before sintering

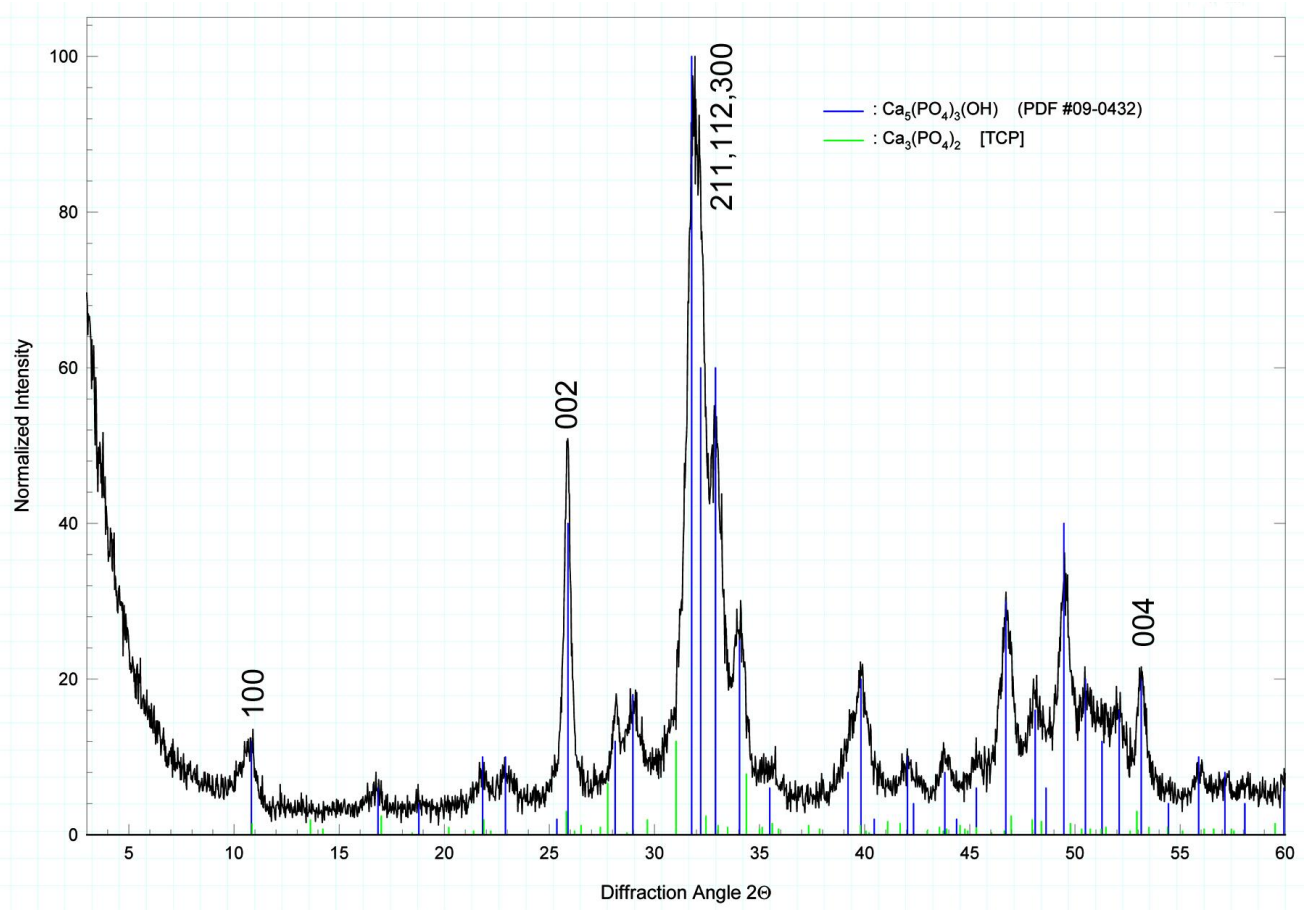

A-1. Before sintering, the major calcium phosphate phase in the mineralized collagen matrix is apatite. The characteristic *hkl* planes of apatite: 100, 002, 211, 112, 300 and 004 are depicted on top of the spectrum. A small peak at 2Θ = 31 degrees appears to be beyond what may be considered as noise. This small peak may represent minute traces of tricalcium phosphate. However, there is no peak at 2Θ = 4.9 degrees that is characteristic of octacalcium phosphate (see peak designations in A-2).

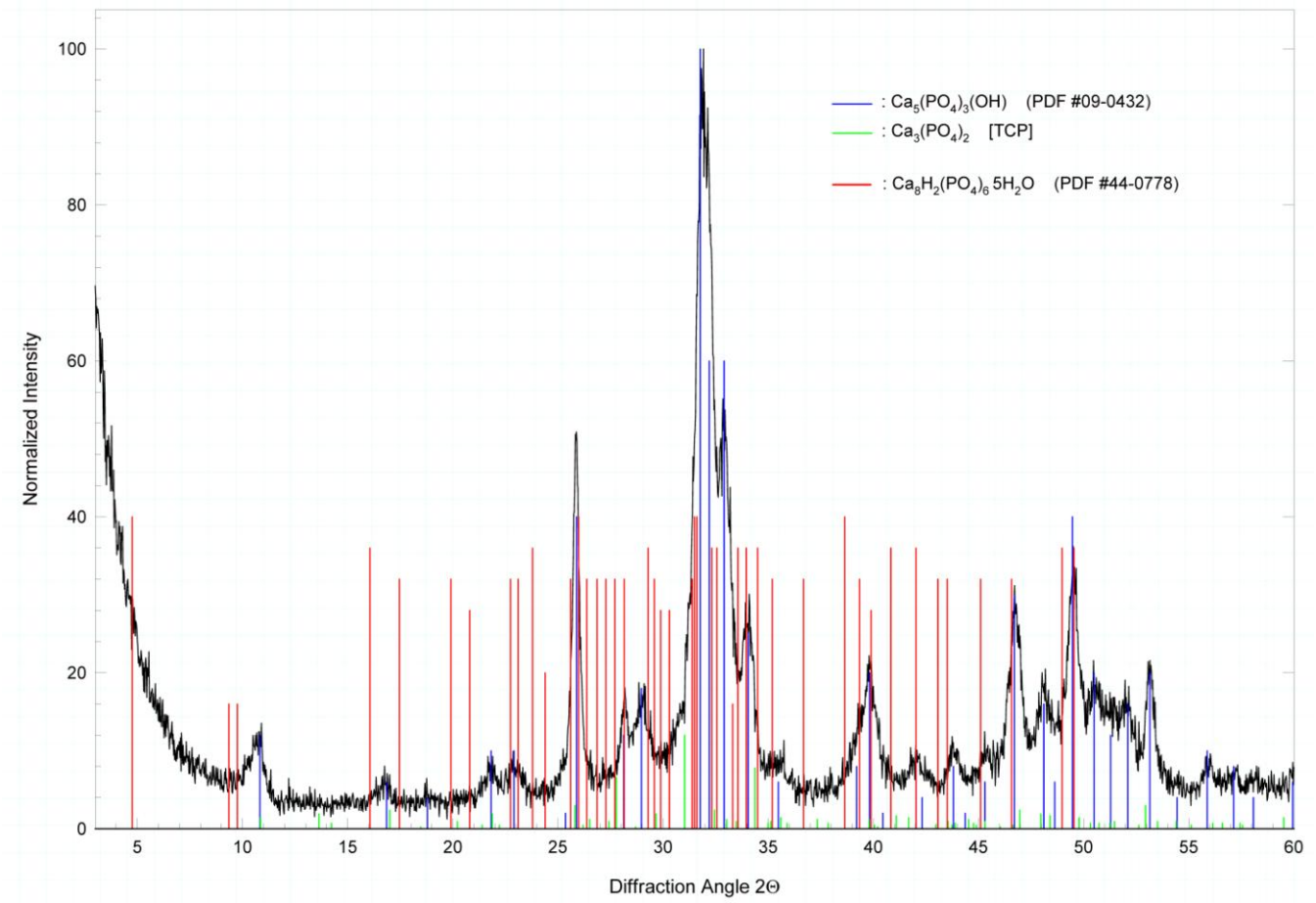

A-2. Same spectrum as A-1, with peak designations for octacalcium phosphate superimposed in red.

B. After sintering

The crystallinity of apatite derived from the mineralized collagen matrix powder increased after sintering, as indicated by the narrowing and sharpening of the diffraction peaks. Lack of a peak at 2Θ = 4.9 degrees is indicative of the absence of octacalcium phosphate. Calcium oxide is derived from the calcium hydroxide released by the Portland cement.

… contd. next page

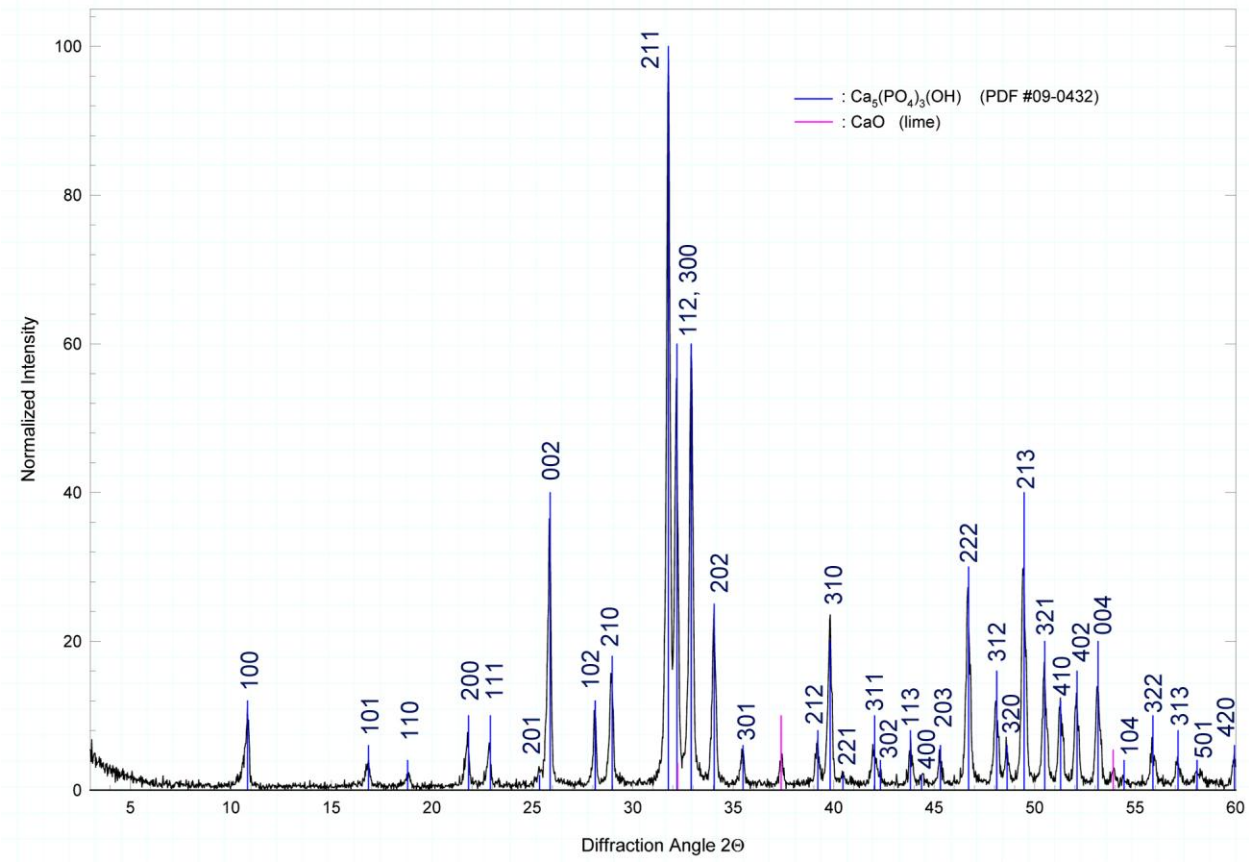
: $Ca_5(PO_4)_3(OH)$ (PDF #09-0432)
: CaO (lime)
Normalized Intensity
Diffraction Angle 2Θ
100
101
110
200
111
201
002
102
210
211
112, 300
202
301
212
310
221
311
302
113
400
203
222
312
320
213
321
410
402
004
104
322
313
501
420

SI-8: References for Supporting Information

(S1) Sonawane, S. H.; Gumfekar, S. P.; Meshram, S.; Deosarkar, M. P.; Mahajan, C. M.; Khanna, P. *In. J. Chem. React. Eng.* **2009**, *7*, A47.

(S2) Gebauer, D.; Völkel, A.; Cölfen, H. *Science* **2008**, *322*, 1819–1822.

(S3) Dey, A.; Bomans, P.H.; Müller, F.A.; Will, J.; Frederik, P.M.; de With, G.; Sommerdijk, N.A. *Nat. Mater.* **2010**, *9*, 1010-1014.

(S4) Markovic, M.; Fowler, B. O.; Tung, M. S. *J. Res. Natl. Inst. Stand. Technol.* **2004**, *109*, 553–568.